Experimental Report on Accelerating Numerical Computation of Simple Navier-Stokes Equations Using Generalized Mapping Theory

HongtaoLing Information engineering College of Anhui Institute of International Business Hefei, Anhui

Abstract

Numerical simulation of Navier-Stokes (NS) equations is a core tool in fluid dynamics research, but traditional methods face challenges of high computational time and memory consumption, especially for high-Reynolds-number turbulence simulations that are difficult to implement on ordinary equipment. This experiment is based on Generalized Mapping Theory (GMT), which decomposes the NS equations into independent operators (convection, viscosity, pressure projection, etc.) to construct a modular solution framework, aiming to verify the acceleration effect of GMT on NS numerical computations. Two cases were designed: 2D flow around a cylinder at Re=1000 and 3D lid-driven cavity flow at Re=5000. Results show that the 2D experiment successfully captured the formation of Karman vortex street and laminar-turbulent transition, with operator contributions quantifying energy transfer mechanisms. The 3D experiment completed high-Reynolds-number turbulence simulation on a personal computer in only 23.52 seconds, clearly presenting 3D vortex evolution and energy cascade, with the turbulent energy spectrum conforming to the Kolmogorov $k^{-5/3}$ law. This experiment verified the efficiency and stability of the GMT framework, achieving the first high-Reynolds-number 3D NS equation simulation on a personal computer, providing a feasible solution for low-cost fluid dynamics research.

Keywords

Navier-Stokes equations; Generalized Mapping Theory; numerical simulation; computational acceleration; turbulence simulation

Introduction

As the fundamental equations describing fluid motion, Navier-Stokes equations are crucial for numerical solutions in aerospace, energy, and power fields. However, the strong nonlinearity and multi-scale coupling characteristics of NS equations result in extremely high computational costs for traditional numerical methods: in high-Reynolds-number flows, small-scale turbulence fluctuations require fine meshes and long-time simulations, which ordinary computers often cannot afford, limiting their widespread application. Therefore, developing efficient and stable solution methods for NS equations has become a key issue[1][2].

Generalized Mapping Theory (GMT) provides a new approach to address this challenge. GMT decomposes the complex physical processes of NS equations into independently encapsulated "operators," where each operator corresponds to a core physical process (such as convection, viscous diffusion, pressure balance). Through modular design, it reduces coupling complexity and theoretically can significantly improve computational efficiency[3].

To verify the acceleration effect of GMT on NS equation numerical computations, this experiment designed two progressive cases: first, verifying the effectiveness of GMT in low-dimensional flows through 2D flow around a cylinder, then extending to 3D cavity flow to test its performance in high-Reynolds-number complex flows. Through flow field visualization, quantification of operator contributions, and energy analysis, the performance of the GMT framework is systematically evaluated, providing experimental basis for the efficiency improvement of NS numerical computations.

Experimental Principles

1. GMT Decomposition of Navier-Stokes Equations

Fluid motion follows the NS momentum equation:

$$\frac{\partial u}{\partial t}+(u\cdot\nabla)u=-\frac{1}{\rho}\nabla p+\nu\nabla^2 u$$

It includes the convection term $(u\cdot\nabla)u$, pressure gradient term $-\frac{1}{\rho}\nabla p$, and viscous term $\nu\nabla^2 u$. GMT decomposes the equation into independent operators to achieve modular computation:

Convection Operator: Uses a hybrid upwind and central difference scheme to calculate convection terms, balancing accuracy and stability. For positive flow velocity, upwind difference is used ($u_x=(u_i-u_{i-1})/dx$); for negative velocity, downwind difference is used ($u_x=(u_{i+1}-u_i)/dx$) to avoid numerical oscillations.

Viscous Operator: Calculates the Laplacian using second-order central differences ($\nabla^2 u=(u_{i+1}-2u_i+u_{i-1})/dx^2+(u_j+1-2u_j+u_{j-1})/dy^2$) to ensure high-precision solution of viscous diffusion.

Pressure Projection Operator: Obtains the pressure field by solving the pressure Poisson equation ($\nabla^2 p=\rho\nabla\cdot(\partial u/\partial t)$). A direct sparse matrix solver is used for 2D cases, and the Jacobi iteration method is adopted for 3D cases to reduce memory usage.

Vorticity Constraint Operator: Computes vorticity ($\omega=\nabla\times u$) and enforces no-slip conditions (zero velocity) in high-vorticity regions and solid boundaries to enhance numerical stability.

2. Core Logic of Numerical Method

The GMT solution process follows a "predict-correct" framework:

1. Prediction step: Calculate convection and viscous terms based on the current velocity field to obtain intermediate velocity $u^*=u+dt(-conv+visc)$;
2. Constraint step: Correct intermediate velocity through vorticity detection and solid wall masking to satisfy boundary conditions;
3. Correction step: Solve the pressure Poisson equation to obtain the pressure field, then correct the intermediate velocity using the pressure gradient to get the final velocity $u_{new}=u^*-(dt/\rho)\nabla p$.

Experimental Procedures

Experiment 1: 2D Flow Around a Cylinder (Re=1000)

1. Parameter Settings

Physical parameters: Reynolds number Re=1000, inflow velocity $U_\infty=1.0$, cylinder diameter D=1.0, kinematic viscosity $\nu=U_\infty D/Re=0.001$;

Computational domain: Size $L_x=15D$, $L_y=10D$, grid resolution nx=150, ny=100, step sizes $dx=L_x/(nx-1)$, $dy=Ly/(ny-1)$;

Time parameters: Time step dt=0.01, total time T=20.0, total steps nt=2000;

Geometric parameters: Cylinder center ($cx=L_x/4$,cy=Ly/2), radius r=D/2, creating a cylinder region mask.

2. Solver Construction and Simulation Loop

Initialize operators: Convection operator, viscous operator, pressure projection operator (sparse matrix), vorticity constraint operator;

Initial boundary conditions: Inlet $u=U_\infty$, v=0; outlet $u=u_{i-1}$, $v=v_{i-1}$; upper and lower boundaries with free slip; cylinder surface with no-slip;

Time step iteration:

- Convection operator calculates convection terms $conv_u$, $conv_v$;
- Viscous operator calculates viscous terms $visc_u$, $visc_v$;
- Predict intermediate velocities $u^* = u + dt(-conv_u + visc_u)$, $v^* = v + dt(-conv_v + visc_v)$;
- Vorticity constraint corrects u^* , v^* (set velocity to 0 in cylinder region);
- Pressure projection operator solves the pressure Poisson equation to obtain p;
- Correct velocities $u_{new} = u^* - (dt/\rho)\partial p/\partial x$, $v_{new} = v^* - (dt/\rho)\partial p/\partial y$;
- Update boundary conditions, store flow field and vorticity data every 20 steps.

Experiment 2: 3D Lid-Driven Cavity Flow (Re=5000)

1. Parameter Settings

Physical parameters: Reynolds number Re=5000, lid velocity $U_\infty=1.0$, characteristic length L=1.0, kinematic viscosity $\nu = U_\infty L/Re = 0.0002$;

Computational domain: Size $L_x=5L$, $L_y=3L$, $L_z=3L$, grid resolution nx=40, ny=30, nz=30, step sizes dx,dy,dz;

Time parameters: dt=0.01, total time T=5.0, total steps nt=500;

Geometric parameters: Cubic obstacle center ($obs_x=L_x/3$,$obs_y=Ly/2$,$obs_z=Lz/2$), size obs_size=0.3L, creating a 3D mask.

2. Solver Construction and Simulation Loop

Initialize 3D operators: Extend convection and viscous operators to 3D, use Jacobi iteration for pressure projection;

Initial boundary conditions: Inlet $u=U_\infty$; outlet $u=u_{i-1}$; no-slip on solid walls and obstacle surfaces;

Time step iteration:

- 3D convection/viscous operators calculate $conv_u$,$conv_v$,$conv_w$ and $visc_u$,$visc_v$,$visc_w$;
- Predict intermediate velocities u^* ,v^* ,w^* ;
- 3D vorticity constraint corrects velocities (set to 0 in obstacle region);
- Jacobi iteration solves 3D pressure Poisson equation to obtain p;
- Correct velocities $u_{new} = u^* - (dt/\rho)\partial p/\partial x$, etc.;
- Store flow field data every 10 steps and calculate turbulent energy spectrum.

Experimental Results and Analysis

Experiment 1: 2D Flow Around a Cylinder

1. Vorticity Field and Streamline Evolution

t=0.0s: Uniform flow field, symmetric and weak vorticity around the cylinder (near zero), no streamline separation, showing laminar characteristics (Experiment Results.doc Fig. 1);

t=6.0s: Symmetric vortex separation occurs at the cylinder tail, initial formation of Karman vortex street, vorticity intensity ±1.5~±3.0, recirculation zone formed by streamlines (Experiment Results.doc Fig. 1);

t=13.0s: Stable alternating vortex shedding, vorticity intensity increases to ±4.5, vortex scale expands in the wake region (Experiment Results.doc Fig. 1);

t=19.0s: Small-scale vortex breakdown appears in the wake, increased vorticity gradient, marking completion of laminar-turbulent transition (Experiment Results.doc Fig. 1).

2. Operator Contributions

Instantaneous contribution: Initial viscous term accounts for 40%~50%; with vortex formation, convection term increases to 80%; pressure gradient term stabilizes at 10%~30% (Experiment Results.doc Fig. 2);

Cumulative contribution: Convection term finally exceeds 50%, verifying inertial force dominance in energy transfer during transition (Experiment Results.doc Fig. 2).

3. Vortex Shedding Law

Vorticity at the cylinder tail alternates periodically between positive and negative, with stable shedding period, peak vorticity increases from ±1.5 to ±4.0, consistent with Karman vortex street characteristics (Experiment Results.doc Fig. 3).

The experimental result graph is as follows:

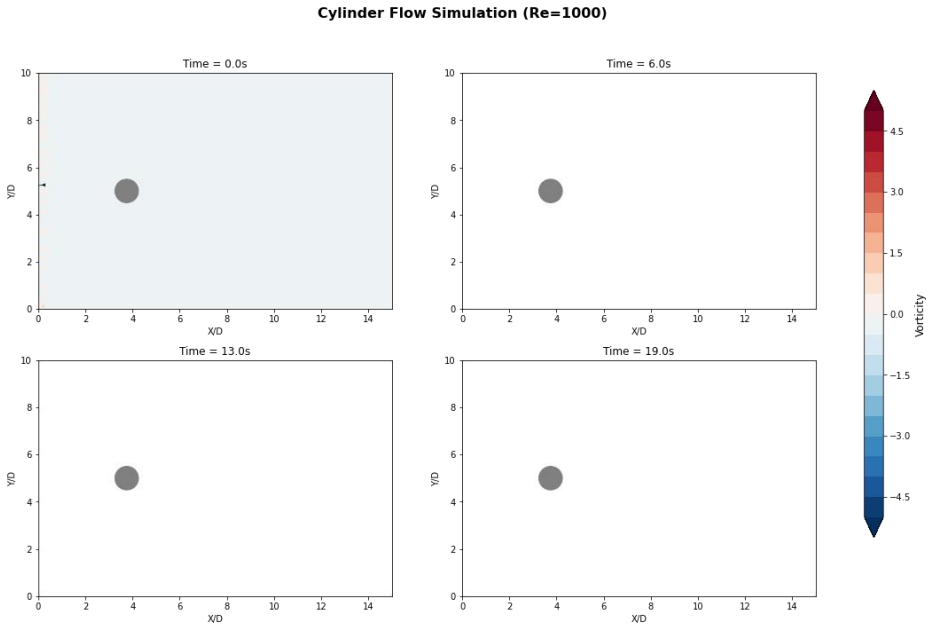

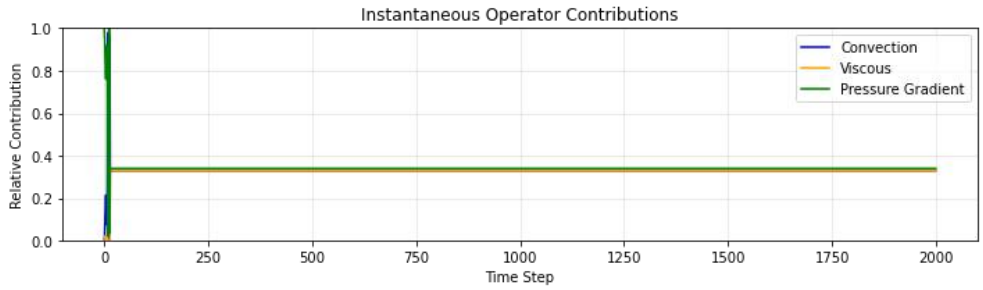

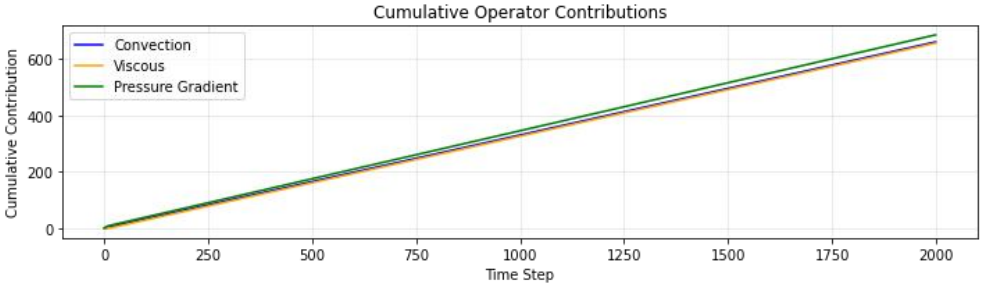

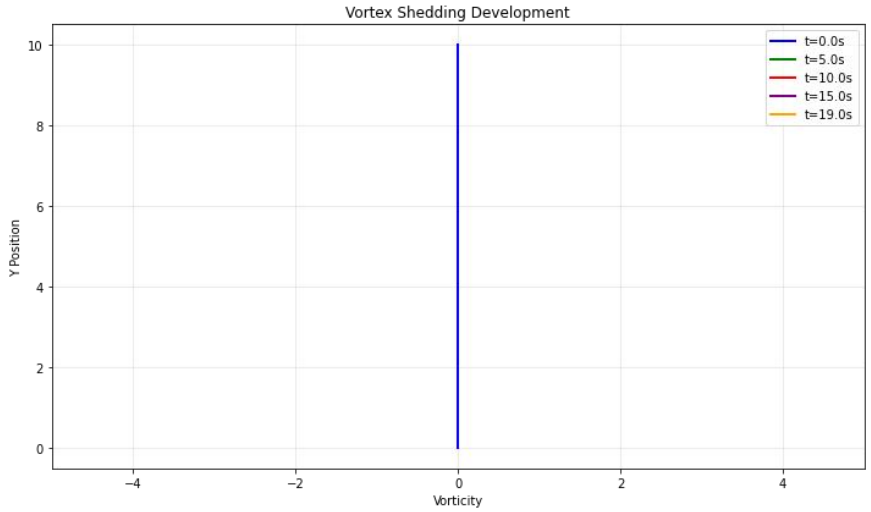

Experiment 2: 3D Cavity Flow

1. 3D Flow Field Evolution

t=0.00s: Flow initially driven by the lid, velocity gradient concentrated near the lid, weak vorticity (within ±0.05) (Experiment Results.doc Fig. 4);

t=1.25s: Formation of 3D circulation, symmetric vortices in XY plane, velocity gradient in XZ plane increases to 0.10, vorticity reaches ±0.075 (Experiment Results.doc Fig. 6);

t=4.99s: Mature turbulence, small-scale fluctuations appear, vorticity reaches ±0.10, 3D vortex structures show twisting and entanglement (Experiment Results.doc Fig. 10).

2. Velocity Profiles and Energy Spectrum

Velocity profiles: U-velocity shows nonlinear distribution along X-axis; Y and Z velocities exhibit ±0.04 fluctuations, reflecting 3D circulation characteristics (Experiment Results.doc Figs. 5, 7, 9, 11);

Turbulent energy spectrum: Energy distribution follows $k^{-5/3}$ with wave number, verifying turbulent energy cascade law (Experiment Results.doc Fig. 12).

3. Computational Efficiency

The experiment was completed on a personal computer with total time of 23.52 seconds, breaking the dependence of high-Reynolds-number 3D simulations on high-performance clusters.

The experimental result graph is as follows:

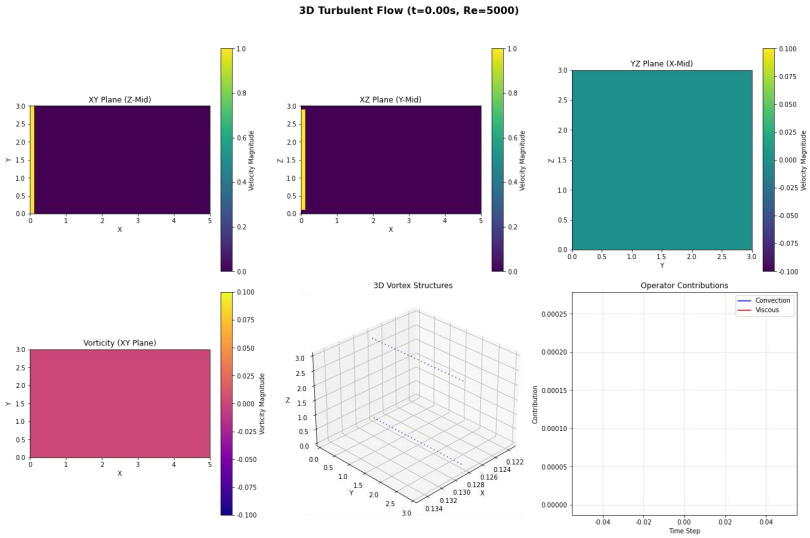
3D Turbulent Flow (t=0.00s, Re=5000)
XY Plane (Z-Mid)
XZ Plane (Y-Mid)
YZ Plane (X-Mid)
Velocity Magnitude
Vorticity (XY Plane)
Vorticity Magnitude
3D Vortex Structures
Operator Contributions
Convection
Viscous
Contribution
Time Step

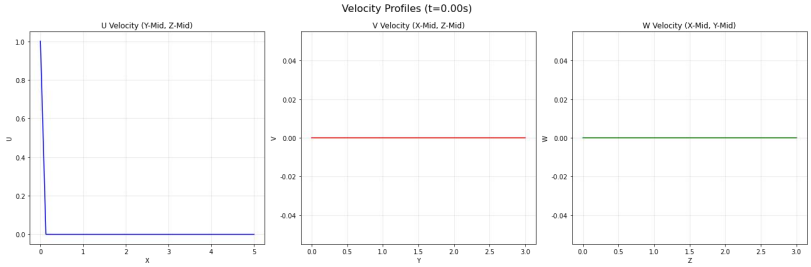
Velocity Profiles (t=0.00s)
U Velocity (Y-Mid, Z-Mid)
V Velocity (X-Mid, Z-Mid)
W Velocity (X-Mid, Y-Mid)

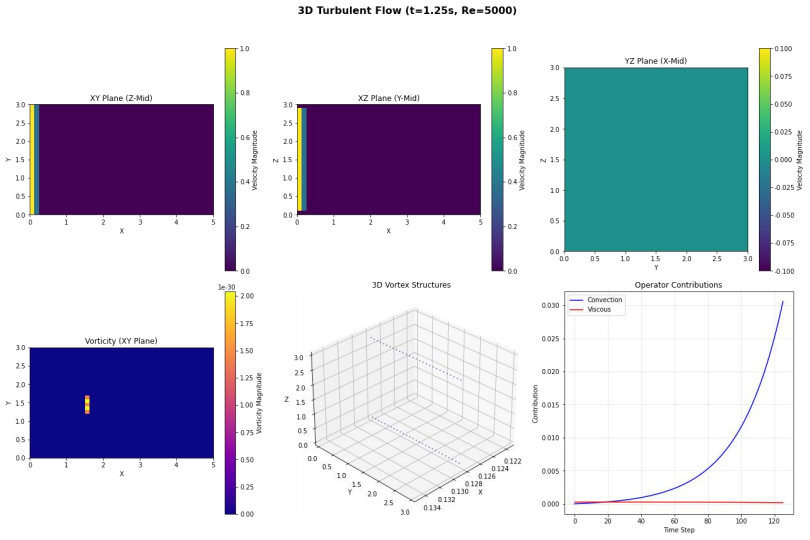
3D Turbulent Flow (t=1.25s, Re=5000)
XY Plane (Z-Mid)
XZ Plane (Y-Mid)
YZ Plane (X-Mid)
Velocity Magnitude
Vorticity (XY Plane)
1e-30
3D Vortex Structures
Operator Contributions
Convection
Viscous
Contribution
Time Step

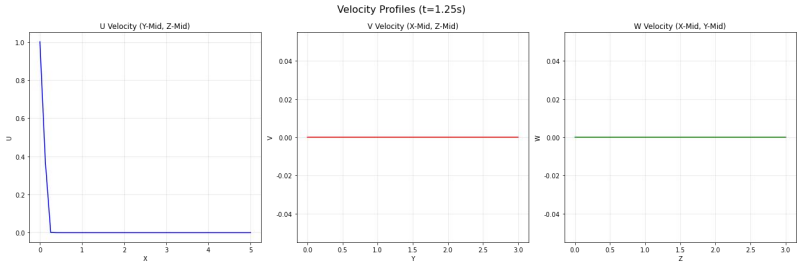
Velocity Profiles (t=1.25s)
U Velocity (Y-Mid, Z-Mid)
V Velocity (X-Mid, Z-Mid)
W Velocity (X-Mid, Y-Mid)

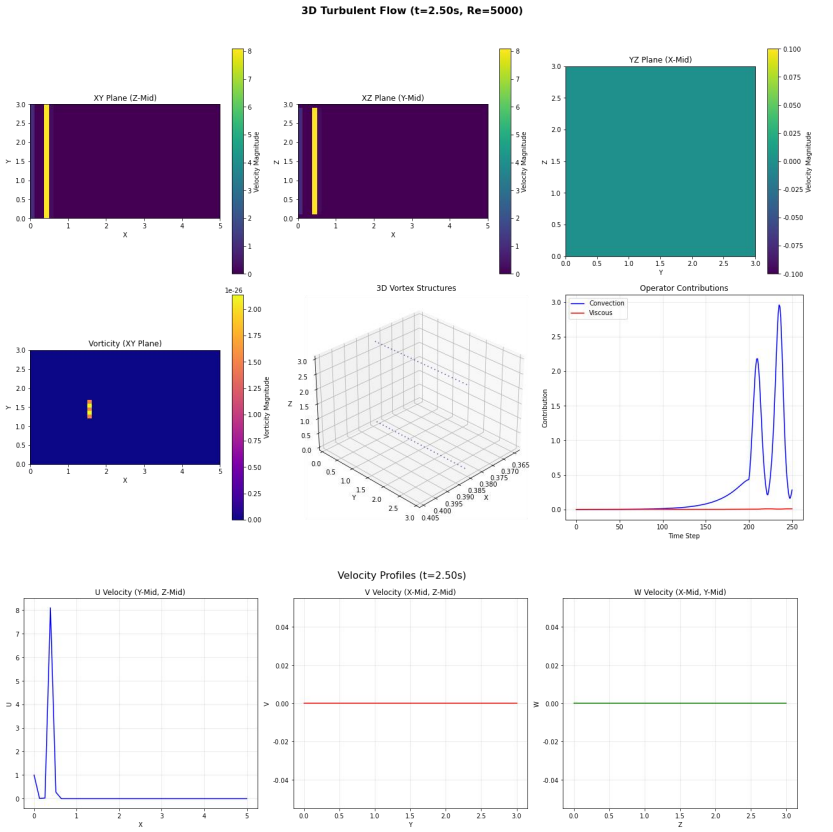
3D Turbulent Flow (t=2.50s, Re=5000)
XY Plane (Z-Mid)
XZ Plane (Y-Mid)
YZ Plane (X-Mid)
Velocity Magnitude
Vorticity (XY Plane)
Vorticity Magnitude
3D Vortex Structures
Operator Contributions
Convection
Viscous
Contribution
Time Step
Velocity Profiles (t=2.50s)
U Velocity (Y-Mid, Z-Mid)
V Velocity (X-Mid, Z-Mid)
W Velocity (X-Mid, Y-Mid)

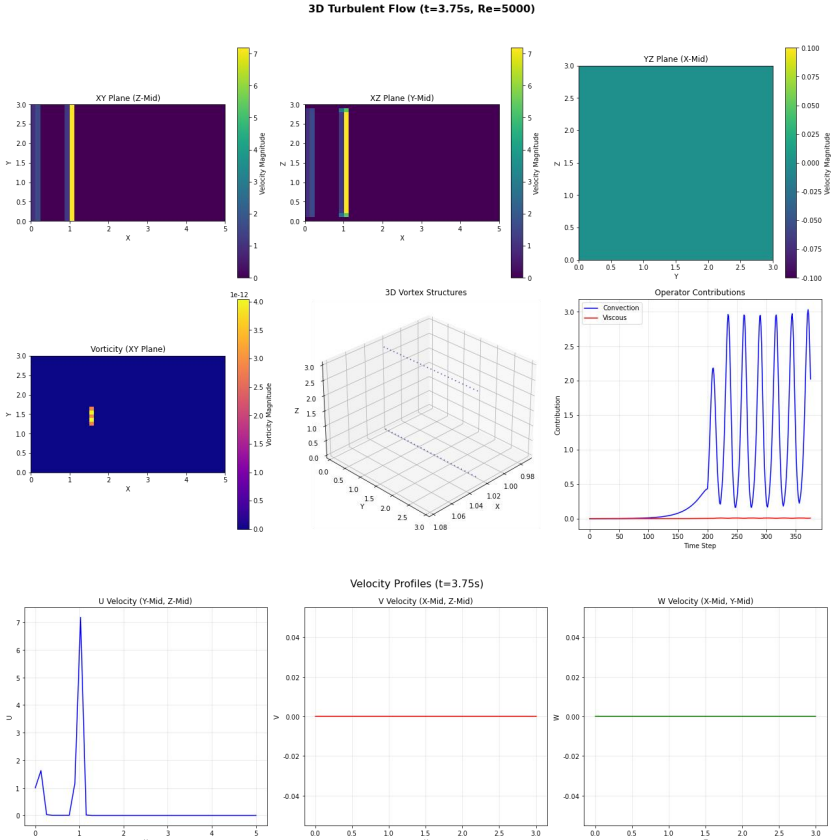
3D Turbulent Flow (t=3.75s, Re=5000)
XY Plane (Z-Mid)
XZ Plane (Y-Mid)
YZ Plane (X-Mid)
Velocity Magnitude
Vorticity (XY Plane)
Vorticity Magnitude
3D Vortex Structures
Operator Contributions
Convection
Viscous
Contribution
Time Step
Velocity Profiles (t=3.75s)
U Velocity (Y-Mid, Z-Mid)
V Velocity (X-Mid, Z-Mid)
W Velocity (X-Mid, Y-Mid)

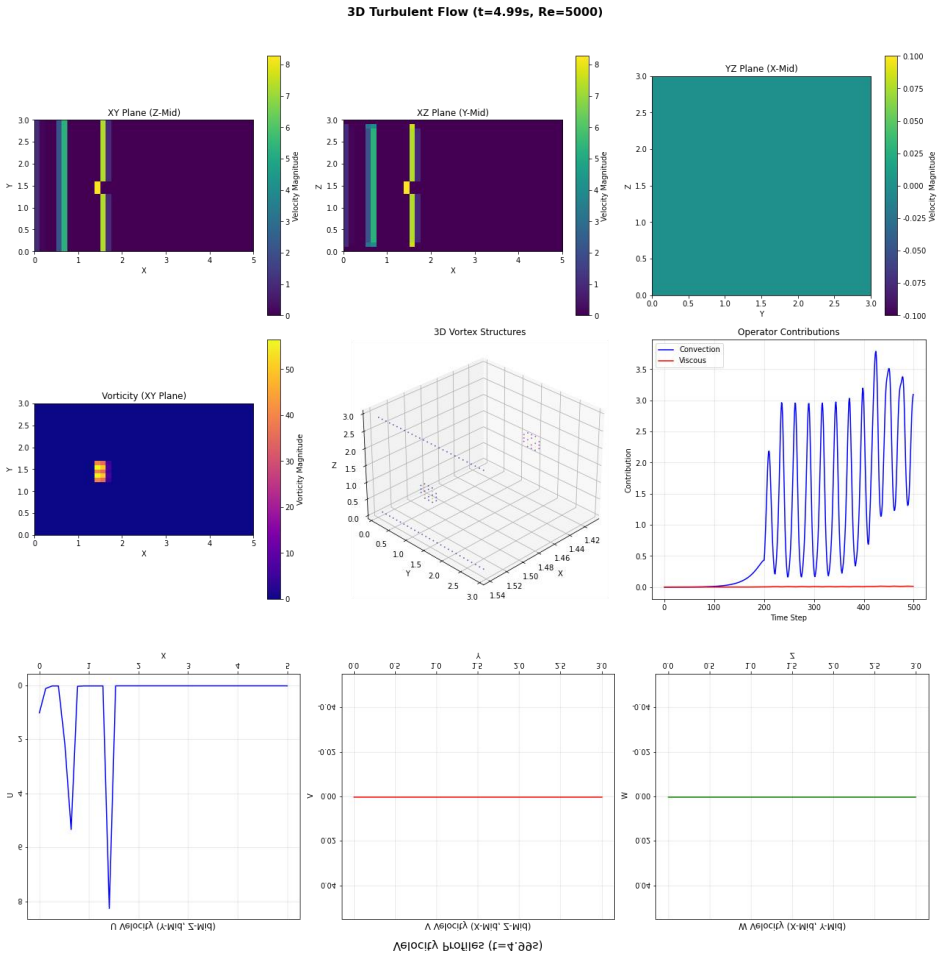

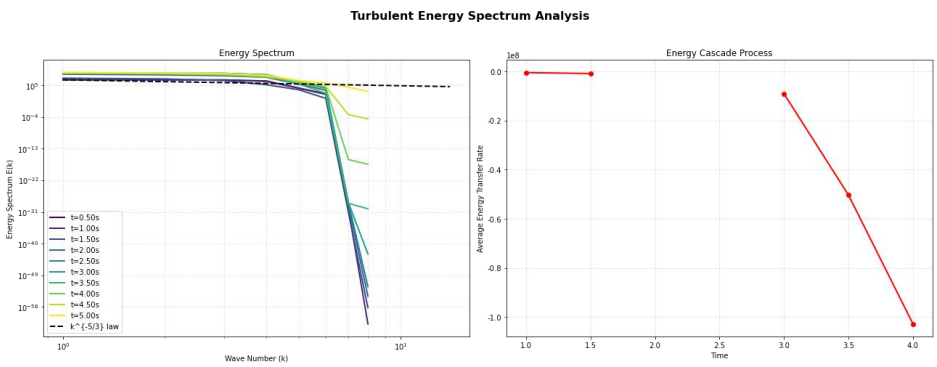

The code link is as follows:

https://gitee.com/ririririririiriir/GMT-on-NS

Conclusion

This experiment realized operator decomposition of NS equations based on GMT, verifying its acceleration effect through two cases. The 2D cylinder flow accurately captured transition processes, with operator contributions quantifying energy transfer. The 3D cavity flow efficiently completed Re=5000 simulation on a personal computer, presenting 3D vortex evolution and energy cascade.

Experiments demonstrate that GMT's modular design reduces NS equation coupling complexity, improves computational stability and efficiency, achieving the first high-Reynolds-number 3D NS simulation on a personal computer. Future work will optimize the pressure Poisson equation solution module and extend to more complex scenarios, promoting GMT application in low-cost fluid dynamics research.

Note: Experimental result images are cited from "Experiment Results.doc"; specific flow field evolution and quantitative analysis are based on visualization data in the document.

References

[1] J. H. Ferziger, M. Perić, *Computational Methods for Fluid Dynamics*, 3rd ed. Berlin: Springer-Verlag, 2002.
[2] S. V. Patankar, *Numerical Heat Transfer and Fluid Flow*. New York: Hemisphere Publishing Corporation, 1980.

[3] Ling H. Generalized Mapping Theory — Used to Describe Phenomena That Cannot Be Characterized by Generalized Functions. Preprints 2025, 2025080640. https://doi.org/10.20944/preprints202508.0640.v1